Physics of the Solid State, 2025, Vol. 67, No. 2

11

Graphene on ferromagnetic isolator EuX (X = O, S, Se, Te)

© *S.Yu. Davydov*

Ioffe Institute,
St. Petersburg, Russia

E-mail: Sergei_Davydov@mail.ru

Received January 20, 2025
Revised February 4, 2025
Accepted February 12, 2025

A simple model of the density of states of EuX is proposed, taking into account the p bands of the X atoms, the $4f$ and $6s$ bands of the Eu atoms. Within the framework of this model, the influence of the substrate on the single-layer graphene is determined: it turned out that the p band of X plays the main role. Analytical expressions are obtained for the charge transfer between graphene and europium chalcogenide and the magnetization of graphene induced by the Zeeman exchange field of europium atoms.

Keywords: Adsorption approach, broadening and shift of graphene electron states, charge transfer, magnetization of graphene.

DOI: 10.61011/PSS.2025.02.60689.14-25

1. Introduction

A question concerning the possibility of magnetic states in carbon structures arose as early as in the „pre-graphene age" [1–3] and the discussion continued [4–6] until this possibility was more recently proved experimentally on the graphene nanoribbon edges [7]. Since that time, it has been commonly believed that magnetic states of graphene shall be sought for in situations when the structure of an ideal infinite graphene layer is disturbed, which, however, prevents from using such graphene in spintronics and quantum computers. Therefore, it is natural that magnetization is induced in the epitaxial graphene (epigraphene) by magnetic substrate, i. e. due to proximity effect. A simple scheme for describing the induced magnetization in epigraphene due to the contact with ferromagnetic metal (FM) was proposed in [8,9]. Here, the same scheme will be first applied to single layer graphene (SLG) on the surface of a ferromagnetic insulator (FMI), for which monochalcogenides EuX, where X = O, S, Se, Te, were used.

Investigations of the properties of these compounds started from the late 1960s [10–13]; ab initio calculations are described in [14–16]. Focus has been recently made on heterostructures involving EuS: SLG/EuS [17], InAs/EuS [18] and BLG (bilayer graphene)/$\mathrm{Cr_2X_2Te_6}$, where X = Se, Si, Sm [19]. It is estimated that EuS is characterized by a considerable exchange interaction constant $J_{\mathrm{ex}} \sim 10\,\mathrm{meV}$ and large magnetic moment $\sim 7\mu_{\mathrm{B}}$ per Eu ion.

2. Model of density of states for EuX

A fairly simple, but adequate model of the density of states of a substrate is the key element of the adsorptive approach to the description of epilayer electron spectrum [20]. Actually, given Green's function of free-standing graphene is written as $g(\omega, \mathbf{q}) = (\omega - \varepsilon_{\mathbf{q}} + i0^{+})^{-1}$, where ω is the energy variable, $\varepsilon_{\mathbf{q}}$ is the electron dispersion law, $\mathbf{q}$ is the 2D wave vector. Then Green's function of epigraphene may be given by

$$G_{\sigma}(\omega, \mathbf{q}) = \big(\omega - \varepsilon_{\mathbf{q}} - \Sigma_{\sigma}(\omega)\big)^{-1}. \tag{1}$$

Here, σ is the spin index, $\Sigma_{\sigma}(\omega) = \Lambda_{\sigma}(\omega) - i\Gamma_{\sigma}(\omega)$ is the self-energy part, $\Gamma_{\sigma}(\omega) = \pi V^{2}(\omega)\rho_{\sigma}^{\mathrm{sub}}(\omega)$ is the graphene state broadening function and $\Lambda_{\sigma}(\omega)$ is the state shift function, which is the Hilbert transform of $\Gamma_{\sigma}(\omega)$, $\rho_{\sigma}^{\mathrm{sub}}(\omega)$ is the density of states of the substrate, $V(\omega)$ is the matrix element of interaction between the graphene and substrate (dependence on ω will be explained below). Thus, the problem at this stage reduces to setting the density of states of the substrate.

Energy band diagrams for EuX compounds are shown in [10–13], energy bands are shown in [14–17]. According to these works, the electronic spectrum of EuX compounds has three typical continuous spectrum bands: 1) valence band formed by the p-states of chalcogenides in the energy interval $E_{\nu}^{-} = -W_{\nu}/2 \le \Omega_{\nu} \le W_{\nu}/2 = E_{\nu}^{+}$, where $\Omega_{\nu} = \omega - \overline{\omega}_{\nu}$, W_{ν} is the valence band width, the center of which is corresponded by $\overline{\omega}_{\nu}$; 2) conduction band formed by $6s$- and $5d$ states, and by hybridized p-states of X, whose energy interval is given by the same expressions as for the valence band, but with ν replaced with c; 3) f-state band subband fully filled by 7 electrons for spin $\sigma = \downarrow$ is located in the energy interval $E_{c}^{-} - E_{\nu}^{+}$ defined by $E_{f\downarrow}^{-} = -W_{f}/2 \le \Omega_{f\downarrow}/2 = E_{f\downarrow}^{+}$; center of the empty subband $\overline{\omega}_{f\uparrow}$ is higher by $\sim 10\,\mathrm{eV}$ than $\overline{\omega}_{f\downarrow}$ and is deep in the conduction band; the band gap means $E_{g} = E_{c}^{-} - E_{f}^{+}$ [10], band gap widths, including spin, are shown in [15]. Model densities of states corresponding to these continuous spectrum bands schematically shown in Figure 1 (f-subband for spin $\sigma = \downarrow$, and the center and ceiling of the conduction band are not shown in Figure 1). The corresponding energy parameters are shown in the

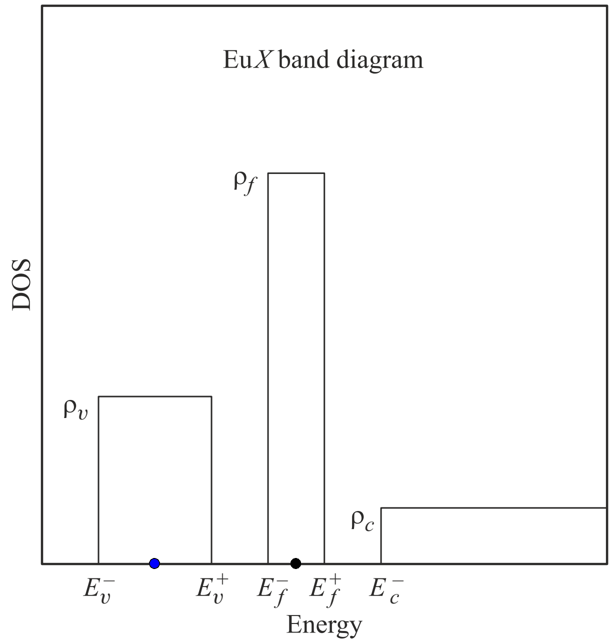

Figure 1. Model densities of states for the valence band $\rho_\nu(\omega)$, filled subband of f-states $\rho_f(\omega)$ (spin index is not specified) and conduction band $\rho_c(\omega)$. Bullets on the energy axis show the centers of the valence band $\overline{\omega}_\nu$, conduction band $\overline{\omega}_c$, the center of the filled f-band $\overline{\omega}_f$ is out of the figure.

table where the values of work functions φ are also added according to [10].

Densities of states shown in Figure 1 correspond to the Friedel model („pedestal" type) [8,9,21]:

$$\rho_{\nu(c)} = \begin{cases} \overline{\rho}_{\nu(c)}, & |\Omega_{\nu(c)}| \le W_{\nu(c)}/2, \\ 0, & |\Omega_{\nu(c)}| > W_{\nu(c)}/2, \end{cases}$$

$$\rho_{f\sigma} = \begin{cases} \overline{\rho}_{f}, & |\Omega_{f\sigma}| \le W_{f}/2, \\ 0, & |\Omega_{f\sigma}| > W_{v}/2, \end{cases} \tag{2}$$

where $\overline{\rho}_{\nu(c,f)} = \text{const}$. Then, the broadening functions are written as $\Gamma_{\nu(c)}(\omega) = \pi V^2_{\nu(c)}\rho_{\nu(c)}(\omega)$ and $\Gamma_{f\sigma}(\omega) = $ $= \pi V^2_{f\sigma}\rho_{f\sigma}(\omega)$ and $\Gamma_{\nu(c)}(\omega) = \pi V^2_{\nu(c)}\rho_{\nu(c)}(\omega)$, where $V_{\nu(c,f)}$ is the matrix element of interaction between the valence band states (conduction band, f-band) with p_z-states of graphene (that's what was denoted as $V(\omega)$ **above**). The corresponding shift functions are

$$\Lambda_{\nu(c)}(\omega) = \overline{\Lambda}_{\nu(c)} \ln\left|\frac{\Omega_{\nu(c)} + W_{\nu(c)}/2}{\Omega_{\nu(c)} - W_{\nu(c)}/2}\right|,$$

$$\Lambda_{f\sigma}(\omega) = \overline{\Lambda}_{f} \ln\left|\frac{\Omega_{f\sigma} + W_{f}/2}{\Omega_{f\sigma} - W_{f}/2}\right|, \tag{3}$$

where $\overline{\Lambda}_{\nu(c,f)} = \overline{\rho}_{\nu(c,f)} V^2_{\nu(c,f)}$.

Let's turn to numerical evaluations of $V_{\nu(c)}$ of σ-bond between p_z-states of carbon and $2p$-states of X and $6s$-states of Eu equal to, respectively, $V_{pp\sigma} = 2.22(\hbar^2/m_e d^2)$ and $V_{sp\sigma} = 1.42(\hbar^2/m_e d^2)$, where $\hbar$ is the reduced Planck constant, m_e is the electron weight, d is the distance from the graphene sheet to the substrate, subscript σ is related to the type of bond, rather than to the spin. Herein, all matrix elements are assumed as positive quantities [22].

For evaluation of V_f, we use the results of [23] assuming that $V_f = V_{pf\sigma} = (3\sqrt{5}/2\pi) \cdot [\hbar^2 (r_p r_f^5)^{1/2}/md^5]$, where $r_p(C) = 6.59\,\text{Å}$ and $r_f = 0.42\,\text{Å}$ [24]. Assuming hereinafter $\overline{\rho}_\nu = 6/W_\nu$, $\overline{\rho}_c = 2/W_c$, $\overline{\rho}_f = 7/W_c$ and $d = 3\,\text{Å}$, we get $V_\nu = 1.87\,\text{eV}$, $\overline{\Lambda}_\nu = 5.64\,\text{eV}$; $V_c = 1.2\,\text{eV}$, $\overline{\Lambda}_c = 0.19\,\text{eV}$; $V_f = 0.017\,\text{eV}$, $\overline{\Lambda}_f = 0.002\,\text{eV}$.

Figure 2 shows $\Lambda_\nu(\omega)$ and $\Lambda_c(\omega)$ ($\overline{\Lambda}_f/\overline{\Lambda}_c \approx 10^{-2}$): it is apparent that the valence $2p$-band X makes the main contribution to the total shift and broadening of $\overline{\Gamma}_{\nu(c,f)} = \pi\overline{\Lambda}_{\nu(c,f)}$ states of epigraphene (as any adsorbed layer). (It should be specified here that, by making such statement, the band boundaries, where the shift functions corresponding to these bands undergo logarithmic divergences, are ignored by default).

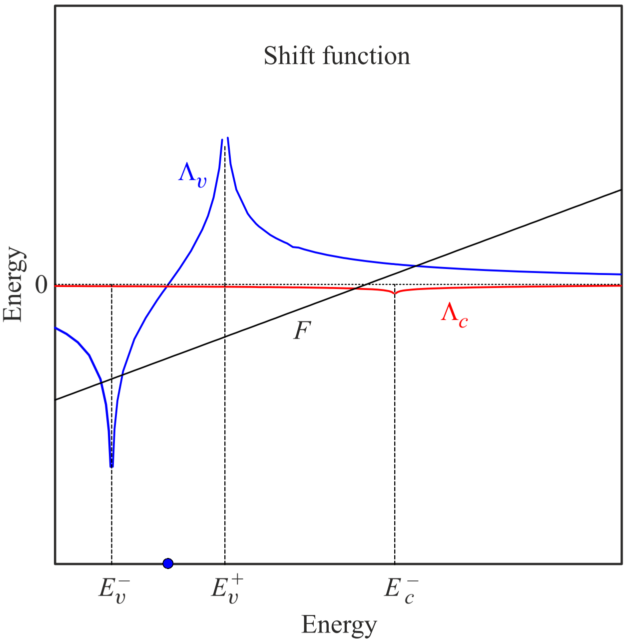

Figure 2. Shift functions $\Lambda_\nu(\omega)$ and $\Lambda_c(\omega)$ and graphical solution of equation (7): point of intersection of line $F \propto (\omega - \varepsilon_\text{D})$ and $\Lambda_\nu(\omega)$ defines the renormalized energy of Dirac point ε^*_D. Vertical dashed lines correspond to the band boundaries.

Energy parameters of the EuX energy band diagram and work function in eV

Parameters	W_ν [10]	$E_f - E_\nu^+$ [14]	W_f [13–15]	E_g [10]]	W_c [13,16]	φ [10]
EuO	~ 3	1.12	~ 1	1.1	~ 15	0.6 ± 0.3
EuS	~ 2	1.65	~ 1	1.7	~ 15	3.3 ± 0.3
EuSe	~ 2	1.80	~ 1	1.9	~ 15	2.8 ± 0.3
EuTe	~ 2	2.00	~ 1	~ 2 [16]	~ 15	–

3. Occupation numbers and magnetic moments of epigraphene atoms

Density of states of SLG corresponds to Green's function (1).

$$\rho_\sigma(\omega, \mathbf{q}) \approx \frac{1}{\pi} \frac{\Gamma_\nu(\omega)}{[\omega - \varepsilon_{\mathbf{q}\sigma} - \Lambda_\nu(\omega)]^2 + \Gamma_\nu^2(\omega)}. \qquad (4)$$

Here, the contributions of conduction band and f state band of EuX electrons were discarded. Within the low-energy approximation, assuming that the vector $\mathbf{q}$ is counted off from the Dirac point $\mathbf{K}$, $\varepsilon_{\mathbf{q}\sigma} = \varepsilon_{\mathrm{D}\sigma} \pm 3taq/2$, where, taking into account the Zeeman effect $\varepsilon_{\mathrm{D}\uparrow,\downarrow} = \varepsilon_{\mathrm{D}} \pm h$, ε_{D} is the Dirac point energy, h is the exchange Zeeman energy of a magnetic field induced by the substrate [25], t is the electron hopping integral between the nearest carbon atoms spaced at a.

Let's introduce the occupation numbers

$$n_{\mathbf{q}\sigma} = \int_{-\infty}^{\infty} \rho_\sigma(\omega, \mathbf{q}) f(\omega - \mu) d\omega, \qquad (5)$$

where $f(\omega - \mu)$ is the Fermi–Dirac distribution functions, μ is the chemical potential.

Consider the $T = 0$ case, taking the energy of the center of valence band as zero ($\overline{\omega}_\nu = 0$). Then

$$n_{\mathbf{q}\sigma} = \frac{\overline{\Gamma}_\nu}{\pi} \int_{-\xi}^{\mu} \frac{d\omega}{[\omega - \Lambda_\nu(\omega) - \varepsilon_{\mathbf{q}\sigma}]^2 + \overline{\Gamma}_\nu^2}, \qquad (6)$$

where $\xi = t\sqrt{2\pi\sqrt{3}} \sim 10\,\mathrm{eV}$ is the cut-off energy [20]. Comparing the work function of EuS (3.3 eV) given in the table with the work function of free-standing undoped SLG $\varphi_{\mathrm{SLG}} = 4.5{-}4.6\,\mathrm{eV}$ [26,27] without considering the shift L_ν, transition of electron to graphene could have been suggested, which is wrong (see below).

To derive an expression for the occupation number n_σ in an analytical form, simplifications shall be used because the expressions for $\rho_\sigma(\omega)$ are already very cumbersome [20,28]. Determining the value of the renormalized (due to the interaction with the substrate) energy of Dirac point ε_{D} from equation

$$\omega - \varepsilon_{\mathrm{D}} - \Lambda_\nu(\omega) = 0, \qquad (7)$$

we obtain $\varepsilon_{\mathrm{D}}^* = \varepsilon_{\mathrm{D}} + \Lambda_\nu(\varepsilon_{\mathrm{D}})$.

Graphical solution of equation (7) is shown in Figure 2. Then, replacing the expression in brackets in (6) with $C_\sigma(q) = \varepsilon_{\mathrm{D}\sigma}^* \mp 3taq/2$, we obtain

$$n_{q\sigma} \approx \frac{1}{\pi} \operatorname{arccot} \frac{C_\sigma(q) - \mu}{\overline{\Gamma}_\nu}. \qquad (8)$$

According to the data in Table and Figures 1 and 2, we obtain $(\varepsilon_{\mathrm{D}} - \overline{\omega}_\nu) \approx 3{-}4\,\mathrm{eV}$, so that $(\varepsilon_{\mathrm{D}}^* - \overline{\omega}_\nu) \approx 7\,\mathrm{eV}$. Thus, under the action of the substrate, the Dirac point shifts to the conduction band region of EuX, consequently, graphene acquires a positive charge. However, only a part of the graphene valence band is filled. Unfortunately, any experimental data concerning carbon adsorption on EuO are not available. It should be emphasized that the adsorption and epitaxial layer theory, treats $\overline{\Gamma}_\nu$ as a fitted parameter [29]. Note, however, that the charge transition, rather than charge direction (sign), depends on $\overline{\Gamma}_\nu$.

We'll further need the values of

$$n_\sigma = N^{-1} \sum_{\mathbf{q}} n_{\mathbf{q}\sigma},$$

where N^{-1} is the number of states $|\mathbf{q}\sigma\rangle$, is the occupation number $n = n_\uparrow + n_\downarrow$ that defines charge transition between SLG and EuX, and substrate-induced epigraphene magnetization $m = n_\uparrow - n_\downarrow$. Expressions needed for calculation are given in the Appendix. Since these expressions are very cumbersome, then a special case is considered here, which illustrates the general situation quite well. Assuming that $aq_{\max} \ll 1$, (8) is written as

$$n_{q\sigma} \approx \frac{1}{\pi} \operatorname{arccot} \frac{C_\sigma(0) - \mu}{\overline{\Gamma}_\nu} \pm \frac{3aq}{2} \frac{t\overline{\Gamma}_\nu}{[C_\sigma(0) - \mu]^2 + \overline{\Gamma}_\nu^2}. \qquad (9)$$

Since only linear terms remain in the low-energy approximation to the graphene spectrum description, expression (9) shall be written as

$$n_\sigma \approx \frac{1}{\pi} \operatorname{arccot} \frac{C_\sigma(0) - \mu}{\overline{\Gamma}_\nu}. \qquad (10)$$

Given $|C_\sigma(q) - \mu| \ll \overline{\Gamma}_\mu$, then $n \sim 1 - 2(\varepsilon_{\mathrm{D}}^* - \mu)/\overline{\Gamma}_\nu$, $|m| \sim 2h/\overline{\Gamma}_\nu$.

If $|C_\sigma(q) - \mu| \gg \overline{\Gamma}_\mu$, we have $n \sim 2\overline{\Gamma}_\nu/\pi(\varepsilon_{\mathrm{D}}^* - \mu)$, $|m| \sim 2h\Gamma_\nu/\pi(\varepsilon_{\mathrm{D}}^* - \mu)^2$.

Energy $h = \mu_{\mathrm{B}}H$, where H is the magnetic field strength and $\mu_{\mathrm{B}} = 5.79 \cdot 10^{-2}\,\mathrm{meV/T}$ is the Bohr magneton. Then at $H = 2{-}20\,\mathrm{T}$, we have $h \sim 0.1{-}1\,\mathrm{meV}$, which order-of-magnitude coincident with the estimates in [30,31]. Note that $h = 11\,\mathrm{meV}$ at $H = 200\,\mathrm{T}$ is provided in [25].

4. Conclusion

A simple model of density of states of europium chalcogenides EuX prosed in this work was used to easily derive the substrate-induced broadening function Γ and shift function Λ of epitaxial graphene states. It was clear that the main contribution to Γ and Λ was made by the valence band formed by $6s$-states of X atoms. Due to such simplification of the problem, analytical expressions were derived for charge transition from graphene atoms to the substrate conduction band that (roughly estimated) turned to be large. Zeeman splitting of graphene states was used to evaluate the graphene magnetization induced by a ferromagnetic insulator EuX. Thus, the adsorptive approach [20,29] used to ignore the crystalline interface structure shows promise for describing the proximity effect. Note that the topic of induced magnetization in heterostructures have been gaining popularity over the past five years [32–36].

Conflict of interest

The author declares no conflict of interest.

Appendix

To calculate the occupation numbers and magnetic moments, dimensionless parameters $e_\sigma = \varepsilon^*_{\mathrm{D}\sigma}/\Gamma_V$, $\tau = 3t/2\overline{\Gamma}_\nu$, $\overline{\mu} = \mu/\overline{\Gamma}$, $x = aq$ and an auxiliary integral are introduced

$$I^{\pm}_{\sigma} = 1 + \frac{2}{\tau^2}\int\limits_0^{\tau} \arctan(y + \overline{\mu} - e_\sigma)y\,dy, \tag{A1}$$

where $y_{\max} = \tau a q_{\max} = \tau$, superscripts $\pm y$ of the integral are related to the Zeeman splitting $\pm h$. We represent $I^{\pm}_{\sigma} = 1 + \{I^{\pm}_{\sigma}\}_1 + \{I^{\pm}_{\sigma}\}_2$, where

$$\{I^{\pm}_{\sigma}\}_1 = \frac{2}{\tau^2}\int\limits_{\overline{\mu}-e_\sigma}^{\tau+\overline{\mu}-e_\sigma} \arctan(z)z\,dz$$

$$= \frac{1}{\tau^2}\left((1+z^2)\,\mathrm{arccotan}(z) - z\right)^{\tau+\overline{\mu}-e_\sigma}_{\overline{\mu}-e_\sigma}, \tag{A2}$$

$$\{I^{\pm}_{\sigma}\}_2 = \frac{2(e_\sigma - \overline{\mu})}{\tau^2}\int\limits_{\overline{\mu}-e_\sigma}^{\tau+\overline{\mu}-e_\sigma} \arctan(z)\,dz$$

$$= \frac{2(e_\sigma - \overline{\mu})}{\tau^2}\left(z\arctan(z) + \frac{1}{2}\ln(z^2+1)\right)^{\tau+\overline{\mu}-e_\sigma}_{\overline{\mu}-e_\sigma}, \tag{A3}$$

$z = \tau x + \mu - e_\sigma$. The derived expressions are used to calculate $n = n_\uparrow + n_\downarrow$ and $m = n_\uparrow - n_\downarrow$.

References

[1] M. Fujita, K. Wakabayashi, K. Nakado, K. Kusakabe. J. Phys. Soc. Japen **65**, 1920 (1996).
[2] T.L. Makarova, B. Sundqvist, R. Hohne, P. Esquinazi, Y. Kopelevich, P. Scharff, V.A. Davydov, L.S. Kashevarova, A.V. Rakhma ina. Nature **413**, 716 (2001).
[3] T.L. Makarova. Semiconductors **38**, 615 (2004).
[4] Y.-W. Son, M.L. Cohen, S.G. Louie. Nature **444**, 347 (2006).
[5] O.V. Yaziev. Rep. Prog. Phys. **73**, 056501 (2010).
[6] K. Zollner, M. Gmitra, T. Frank, J. Fabian. Phys. Rev. B **94**, 155441 (2016).
[7] M. Slota, A. Keerthi, W.K. Myers, E. Tretyakov, M. Baumgarten, A. Ardavan, H. Sadeghi, C.J. Lambert, A. Narita, K. Müllen, L. Bogani. Nature **557**, 691 (2018).
[8] S.Yu. Davydov. Phys. Solid State **62**, 378 (2020).
[9] S.Yu. Davydov. Tech. Phys. Lett. **47**, 566 (2021).
[10] D.E. Eastman, F. Holtzberg, S. Methfessel. Phys. Rev. Lett. **23**, 226 (1969).
[11] G. Günterodt. Phys. Cond. Matter **18**, 37 (1974).
[12] A. Mauger, G. Godart. Phys. Rep. **141**, 51 (1986).
[13] P.G. Steeneken, L.H. Tjeng, I. Elfimov, G.A. Sawatzky, G. Ghiringhelli, N.B. Brookes, D.-J. Huang. Phys. Rev. B **88**, 047201 (2002).
[14] D.B. Ghosh, M. De, S.K. De. Phys. Rev. B **70**, 115211 (2004).
[15] M. Horne, P. Strange, W.M. Temmerman, Z. Szotek, A. Svane, H. Winter. J. Phys.: Condens. Matter **16**, 5061 (2004).
[16] P. Larson, W.R.L. Lambrecht. J. Phys.: Condens, Matter **18**, 11333 (2006).
[17] P. Wei, S. Lee, F. Lemaitre, L. Pinel, D. Cutaia, W. Cha, F. Katmis, Y. Zhu, D. Heiman, J. Hone, J.S. Moodera, C.-T. Chen. Nat. Materials **15**, 711 (2016).
[18] Y. Liu, A. Luchini, S. Martí-Saánchez, C. Koch, S. Schuwalow, S.A. Khan, T. Stankevicč, S. Francoual, J.R.L. Mardegan, J.A. Krieger, V.N. Strocov, J. Stahn, C.A.F. Vaz, M. Ramakrishnan, U. Staub, K. Lefmann, G. Aeppli, J. Arbiol, P. Krogstrup. ACS Appl. Mater. Interfaces **12**, 8780 (2020).
[19] K. Zollner, M. Gmitra, J. Fabian. New J. Phys. **20**, 073007 (2018).
[20] S.Yu. Davydov. Phys. Solid State **58**, 804 (2016).
[21] V.Yu. Irkhin, Yu.P. Irkhin. Elektronnaya struktura, fizicheskiye svoystva i korrelyatsionnyye effekty v
[21] d- i f-metallakh i ikh soyedineniyakh. UrO RAN, Ekaterinburg (2004). 472 s. (in Russian).
[22] W.A. Harrison. Phys. Rev. B **27**, 3592 (1983).
[23] W.A. Harrison, G.K. Straub. Phys. Rev. B **36**, 2655 (1087).
[24] G.K. Straub, W.A. Harrison. Phys. Rev. B **31**, 7668 (1985).
[25] I.E. Gobelko, A.V. Rozhkov, D.N. Dresvyankin. JETP Lett. **118**, 676 (2023).
[26] Y.-J. Yu, Y. Zhao, S. Ryu, L.E. Brus, K.S. Kim, P. Kim. Nano Lett. **9**, 3430 (2009).
[27] D. Niesner, T. Fauster. J. Phys.: Condens. Matter **26**, 393001 (2014).
[28] S.Yu. Davydov. Semiconductors **47**, 95 (2013).
[29] S.Yu. Davydov. Theory of Adsorption: Method of Model Hamiltonians (St. Petersburg, LETI, 2013. (in Russian).
[30] H. Haugen, D. Huertas-Hernando, A. Brataas. Phys. Rev. B **77**, 115406 (2008).
[31] T. Tokuyasu, J.A. Sauls, D. Rainer. Phys. Rev. B **38**, 8824 (1988).
[32] T. Norden, C. Zhao, P. Zhang, R. Sabirianov, A. Petrou, H. Zeng. Nat. Commun. **10**, 4163 (2019).
[33] D. Zhong, K.L. Seyler, X. Linpeng, N.P. Wilson, T. Taniguchi, K. Watanabe, M.A. McGuire, K.-M.C. Fu, D. Xiao, W. Yao, X. Xu. Nat. Nanotechnol. **15**, 187 (2020).
[34] L. Ciorciaro, M. Kroner, K. Watanabe, T. Taniguchi, A. Imamoglu. Phys. Rev. Lett. **124**, 197401 (2020).
[35] M. Bora, P. Deb. J. Phys.: Mater. **4**, 034014 (2021).
[36] P.E.F. Junior, T. Naimer, K.M. McCreary, B.T. Jonker, J.J. Finley, S.A. Crooker, J. Fabian, A.V. Stier. 2D Mater. **10**, 034002 (2023).

Translated by E.Ilinskaya